

Quantum critical local spin dynamics near the Mott metal-insulator transition in infinite dimensions

Nagamalleswararao Dasari^{1,*}, N. S. Vidhyadhiraja¹, Mark Jarrell^{2,3}, and Ross H. McKenzie^{4†}

¹Theoretical Sciences Unit, Jawaharlal Nehru Centre For Advanced Scientific Research, Jakkur, Bangalore 560064, India.

²Department of Physics & Astronomy, Louisiana State University, Baton Rouge, LA 70803, USA.

³Center for Computation & Technology, Louisiana State University, Baton Rouge, Louisiana 70803, USA and

⁴School of Mathematics and Physics, University of Queensland, Brisbane 4072, Australia.

Finding microscopic models for metallic states that exhibit quantum critical properties such as ω/T scaling is a major theoretical challenge. We calculate the local dynamical spin susceptibility $\chi(T, \omega)$ for a Hubbard model at half filling using Dynamical Mean-Field Theory, which is exact in infinite dimensions. Qualitatively distinct behavior is found in the different regions of the phase diagram: Mott insulator, Fermi liquid metal, bad metal, and a quantum critical region above the finite temperature critical point. The signature of the latter is ω/T scaling where T is the temperature. Our results are consistent with previous results showing scaling of the dc electrical conductivity and are relevant to experiments on organic charge transfer salts.

A wide range of materials exhibit properties characteristic of strongly correlated electrons. Materials include transition metal oxides [1], cuprates [2], iron based superconductors [3], heavy fermion compounds [4], and organic charge transfer salts [5]. They are particularly interesting because they exhibit emergent quantum states of matter such as unconventional superconductors, spin liquids, and non-Fermi liquid metals. A major challenge is to understand these metallic states which have properties quite distinct from those of simple elemental metals that can be described by Landau Fermi liquid theory. These unusual metallic states mostly occur in close proximity to a Mott insulating phase [1] and/or to a quantum critical point [4]. The concept of quantum criticality may be a useful organising principle [6–8].

Hubbard model is one of the mostly widely studied effective Hamiltonians for strongly correlated electron systems. At the level of Dynamical Mean-Field Theory (DMFT) [9], at half filling and zero temperature there is a first-order phase transition between metallic and Mott insulating phases as the interaction strength U is increased. In a broad region of the $T - U$ phase diagram above the finite temperature critical point associated with the metal-insulator transition it was recently found that the dc electrical conductivity exhibits scaling characteristic of quantum criticality [10–12]. Furthermore, similar scaling was found in experimental data for three different organic charge transfer salts that exhibit a critical point for the Mott transition in the temperature-pressure phase diagram [13]. In this work we show that the local spin dynamics of the Hubbard model calculated with DMFT exhibits ω/T scaling that is characteristic of quantum criticality.

Quantum criticality and ω/T scaling. Varma et al. [14, 15] showed that many of the anomalous properties of the metallic phase of cuprate superconductors at optimal doping can be described as a marginal Fermi liquid with a spin fluctuation spectrum that exhibits ω/T scaling. Finding concrete realistic theoretical microscopic fermion models that exhibit such scaling has proven challenging. Sachdev has reviewed several spin and boson models [6] that exhibit ω/T scaling in the quantum critical region, associated with a quantum critical point. In such systems, the temperature sets the

relevant low temperature scale. For example, for the transverse field Ising model in one dimension ([6], p. 73), the spin dephasing rate $\Gamma = 0.4T$. For the two-dimensional $O(N \geq 3)$ rotor model in the large- N limit, $\Gamma = 0.94T/N$ ([6], p. 142). Parcollet and Georges [16] considered a particular limit of a random Heisenberg model which had a spin liquid ground state and $\chi''(T, \omega)$ exhibited a form consistent with that conjectured in the marginal Fermi liquid scenario. Neutron scattering measurements find that the dynamic spin susceptibility exhibits ω/T scaling for an insulating antiferromagnetic spin chain compound [17] and a Kagome lattice material [18]. Quantum criticality has been found for a Kondo boson-fermion model [19, 20]. This is motivated by experiments on a number of heavy fermion metals [4, 21]. Specifically, inelastic neutron scattering gives the following ω/T scaling, for the wave-vector dependent susceptibility, $\chi''(\omega, \vec{q})^{-1} = T^a F(\omega/T) + \chi'(\omega = 0, \vec{q})^{-1}$ where \vec{q} is the wavevector and the exponent $a = 0.75$.

Our results are summarised in the phase diagram shown in Figure 1. This diagram is deduced from the dynamical spin susceptibility and is similar to that previously found from scaling of the dc electrical conductivity near the critical point the metal-insulator transition [10, 11]. Specifically, there is a quantum critical regime above the critical point; the signature is that the local dynamical spin susceptibility exhibits ω/T scaling. The local spin relaxation rate is linear in temperature, with a value $\Gamma \simeq 0.4T$.

Model Hamiltonian. We study the single band Hubbard model on the Bethe lattice in infinite dimensions and at half filling. The non-interacting density of states is semi-circular with a full bandwidth $W = 2t$. DMFT is used to calculate properties of the model [9]. In the limit of infinite dimensions or of infinite lattice connectivity DMFT is exact. We do not allow for symmetry breaking such as antiferromagnetism. Previously it has been shown that the metallic and Mott insulating phases co-exist in the range, $U_{c1} < U < U_{c2}$, where $U_{c1} = 2.4t$ and $U_{c2} = 2.9t$ [22]. There is a finite-temperature critical point at $U_c = 2.4t$ and $T_c = 0.028t$. Our results at $\beta \equiv 1/T = 70/t$ are consistent with this earlier work (compare Figure 1).

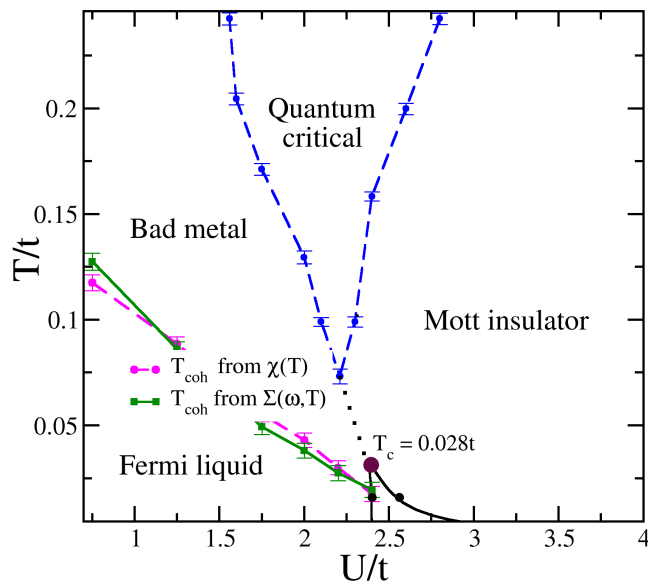


Figure 1. Phase diagram determined from the dynamical spin susceptibility. In the quantum critical region $\chi''(\omega)$ exhibits ω/T scaling with a spin relaxation rate that is proportional to temperature. There is a finite-temperature critical point for the Mott metal-insulator transition ($T_c = 0.028t$). In the Mott insulating phase $\chi''(T, \omega)/\omega$ tends to a delta function peak as the temperature tends to zero. In the Fermi liquid phase the spin relaxation rate is independent of temperature. The coherence temperature for the Fermi liquid was defined in two independent ways. The first where the static spin susceptibility becomes temperature dependent, and the second where the imaginary part of the one-electron self energy $\Sigma''(\omega = 0, T)$ deviates from a T^2 dependence. The black lines define the co-existence region of the metal and Mott insulator, and the critical point, as determined in Ref. 22. Black circles are our results. The blue symbols represent the limits of the quantum critical regime determined by the electron spin relaxation rate plotted in Fig. 2.

Method. The hybridization expansion version of the continuous time quantum Monte-Carlo (CTQMC) [23] is used as a DMFT impurity solver to calculate the spin dynamics at finite temperature. The main advantages of the hybridization expansion CTQMC method are that it is numerically exact and the fermionic sign problem does not occur until very low temperatures in the Fermi liquid regime. The vertex corrected dynamical local spin susceptibility $\chi(\tau) \equiv \langle S_z(\tau)S_z(0) \rangle$ is computed at imaginary times and then Fourier transformed to give values at the Matsubara frequencies on the imaginary frequency axis. It is then determined on the real frequency axis through analytic continuation via the maximum entropy method [24, 25]. As the default model for the analytic continuation we use the closed analytical form results of Salomaa [26] for the resonant level model (Anderson single impurity model with $U = 0$). Given the data, in the Salomaa model the parameter for the width of the spectral density is chosen such that it maximizes the posterior probability of the model. We have also calculated $\chi''(T, \omega)$ by using another default model provided by Bouadim et. al.[27]. We find that our results are independent of the choice of default model, suggesting that

the analytical continuation procedure is quite robust.

Spin relaxation rate. From the local dynamical spin susceptibility, $\chi(T, \omega) \equiv \chi'(T, \omega) + i\chi''(T, \omega)$, a spin relaxation rate can be defined by,

$$\Gamma(U, T) \equiv \lim_{\omega \rightarrow 0} \frac{\omega \chi'(T, \omega = 0)}{\chi''(T, \omega)}. \quad (1)$$

This is similar to the (dephasing) relaxation rate defined by Sachdev for a spin model at the ordering wavevector ([6], page 73). If $\chi(T, \omega)$ has a simple Lorentzian or Drude form then Γ corresponds to the width of the peak at zero frequency in the spectral density, $\chi''(T, \omega)/\omega$. Our results for the temperature dependence of Γ are shown in Figure 2.

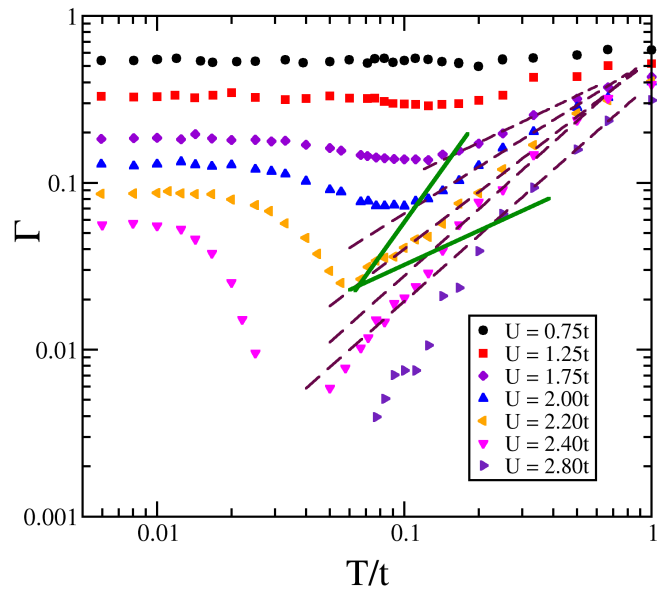


Figure 2. Electron spin relaxation rate $\Gamma(U, T)$ as a function of temperature for different U values. In the Fermi liquid regime of the metallic phase ($T < T_{coh}$) the relaxation rate is non-zero and independent of temperature. This rate decreases by more than an order of magnitude as the Mott insulator is approached. Above the coherence temperature Γ decreases with increasing temperature, reflecting the decreasing interaction between the spins of the electrons which become more localised as the temperature increases. In the Mott insulator ($U > 2.4t$) the rate tends to zero as the temperature tends to zero reflecting the decoupled local moments. In the quantum critical regime the rate is a power law as a function of temperature. For $U = 2.2t$ the rate is approximately linear in temperature, $\Gamma \simeq 0.4T$. The green lines define the boundary of the quantum critical region in Figure 1.

On the metallic side of the Mott transition the signature of the crossover from a Fermi liquid to a bad metal (with increasing temperature above T_{coh}) is that $\Gamma(T, U)$ decreases smoothly from a small T independent value below T_{coh} to a temperature dependent value. Thus in the bad metal the spin dynamics is like the weakly damped dynamics that one would expect if the bad metal was similar to the localised weakly interacting magnetic moments present in the Mott insulating phase. The latter was conjectured to be the character of the

bad metallic state, based on the large entropy and static spin susceptibility found from finite temperature Lanczos calculations for the Hubbard model on the triangular lattice at half filling [28]. We have also determined the coherence temperature from the temperature at which the imaginary part of electronic self energy deviates from the quadratic dependence characteristic of a Fermi liquid (see Figure S1 in the Supplementary Material).

Recent DMFT calculations of charge transport properties of a doped Hubbard model [29] identified the existence of well-defined quasiparticle-like excitations well above the coherence temperature (T_{coh}) and their gradual extinction with the cross-over to the bad metallic regime (T_{MIR}) where the resistivity becomes comparable to the Mott-Ioffe-Regel limit. The transport in this intermediate regime is well described by these resilient quasi-particles (RQPs). Our results in figure 2 are the first study of spin dynamics in the RQP regime which exists at half filling for $U \approx W$. The spin relaxation rate in the RQP regime behaves quite differently in comparison with low temperature Generalized Fermi-liquid and high temperature bad metallic regime. In fact, this might be one of the reasons for the recently observed slowdown of the relaxation dynamics near the Mott transition in the quench dynamics of the Hubbard model[30]. Our results of spin dynamics in the RQP regime open new insights to look at the doped case more carefully since RQP regime is much broader in the temperature window compared with the half-filled band case[29].

Figure 3 shows that above the critical point $\chi''(T, \omega)$ exhibits ω/T scaling characteristic of quantum criticality, i.e. $\chi''(T, \omega) = \chi'(T, \omega = 0)F(\omega/T)$. For low frequencies the scaling function is best fit to a power law, $F(x) = 2.3x$. For $T \gtrsim 0.069t$ the scaling covers about three decades in the ratio ω/T . For comparison, it is shown in the Supplemental Material that in the metallic (Figure S2) and Mott insulating (Figure S3) regions such scaling clearly does not occur. In the Mott insulating phase $\chi''(T, \omega)/\omega$ tends towards a delta function peak, i.e. $\Gamma(T) \rightarrow 0$ as $T \rightarrow 0$ (compare Figure S3). This reflects the decoupled local moments in the Mott phase. In DMFT there is no antiferromagnetic exchange interaction. At zero temperature, the delta function peak is also clearly seen in dynamic DMRG calculations [31].

In boundary conformal field theory (CFT), ω/T scaling is associated with scaling of the imaginary time susceptibility $\chi(\tau)$ as function of $\pi T/\sin(\pi\tau T)$ where τ is the imaginary time [32]. It has been found that such scaling does hold for a Kondo boson-fermion model [19, 20], a fractionalised Fermi liquid in a holographic metal [33], and the gapped single impurity Anderson model [34]. We do not observe such scaling in $\chi(\tau)$ (compare right panel of Figure S4) but do observe such scaling in the one electron local Greens function $G(\tau)$ (compare left panel of Figure S4). Our results illustrate that ω/T scaling does not necessarily imply the scaling characteristic of boundary CFT. The most direct experimental probe of the low frequency behaviour of $\chi(T, \omega)$ is through Nuclear Magnetic Resonance (NMR).

NMR Knight shift. In a lattice system this is given by

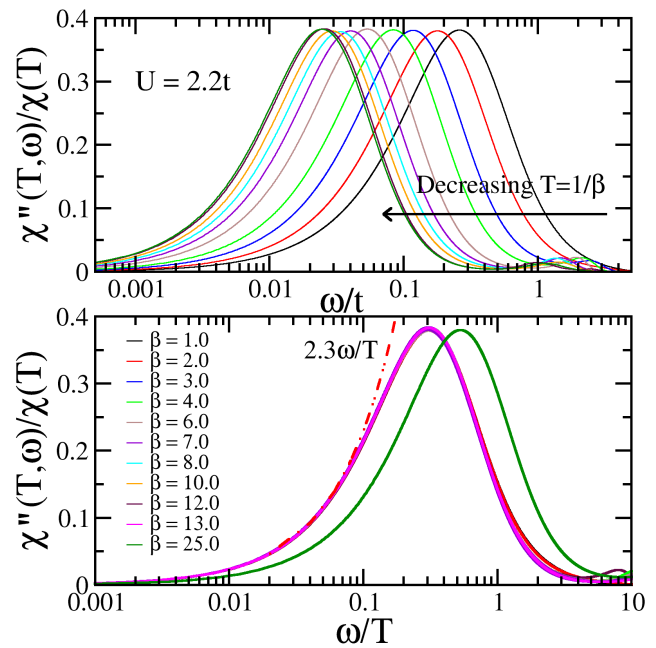


Figure 3. Quantum critical scaling of the dynamical spin susceptibility near the Mott transition. The upper panel shows the frequency dependence of the imaginary part of the susceptibility for $U = 2.2t$ for a range of temperatures ($T = 1/\beta$). The lower panel shows the same data with the frequency scaled by temperature. Scaling occurs for all $T \gtrsim 0.069t$, but fails for $T=0.04t$ (green curve) consistent with the extent of the QC region in Figure 1. The dashed line $2.3\omega/T$ is a best fit to the low frequency data.

$K(T) = A\chi'(\vec{q} = 0, \omega = 0)$, where \vec{q} is the wave vector and A is the hyperfine coupling. Note that the right hand side is not the same quantity as the local spin susceptibility, $\chi'(\omega = 0) \equiv \sum_{\vec{q}} \chi'(\vec{q}, \omega = 0)$, that is our focus here. Nevertheless, for reasons of simplicity, here we do not consider this difference. Figure 4 shows the static local susceptibility as a function of temperature for a range of U values. Here we work with units such that $A = 1$. Note that in the metallic phase as the temperature increases there is a crossover from a temperature independent value at low temperatures, characteristic of a Fermi liquid, to a Curie form $1/(4T)$, characteristic of localised non-interacting spins. The latter occurs in the DMFT treatment of the Mott insulator since it does not include spatial correlations such as the antiferromagnetic interactions due to superexchange.

Nuclear spin relaxation rate. This is given by

$$\frac{1}{T_1 T} = A^2 \lim_{\omega \rightarrow 0} \frac{\chi''(T, \omega)}{\omega} \quad (2)$$

and in a simple Fermi liquid this quantity is independent of temperature (Korringa). Note that there is a relationship to the electron spin relaxation rate Γ defined in equation (1), $T_1 \sim \Gamma/(T\chi'(T, \omega = 0))$. Hence, T_1 being independent of T , which is sometimes associated with quantum criticality [7, 35], is not the same thing as Γ being linear in T , if the temperature dependence of the dc susceptibility is signif-

icant (as it is here). Figure 4 shows $1/(T_1T)$ as a function of temperature for a range of U values. Below the coherence temperature for the metallic phase it is independent of temperature, as expected. Its magnitude is significantly enhanced as the Mott insulator is approached. For comparison, we note that Zitko, Osolin, and Jeglic [36] calculated $\chi''(T, \omega)/\omega$ for a doped Hubbard model at filling $n = 0.8$ using the numerical renormalisation group as an impurity solver in DMFT. They found that $1/T_1$ was a non-monotonic function of temperature and increased by up to two orders of magnitude as U/W increased from 0 to 4, and was weakly temperature dependent in the bad metal regime.

Korringa-Shiba relation. In a simple Fermi liquid the following dimensionless ratio is unity [37],

$$\kappa(T) \equiv \lim_{\omega \rightarrow 0} \frac{\chi''(T, \omega)}{2\pi\omega\chi'(T, \omega)^2}. \quad (3)$$

Shiba [38] showed that for the single Anderson impurity model $\kappa(T) = 1$ in the Kondo regime. Values of κ larger and less than one are often associated respectively with antiferromagnetic and ferromagnetic fluctuations. In Figure 4 we plot this ratio as a function of temperature for a range of U , and find that it is much larger than unity and increases as the Mott insulating phase is approached from the metallic side. In the Fermi liquid regime, κ is close to one.

Comparison with experimental results for organic charge transfer salts. The materials that are arguably closest to the model considered here are the organic charge transfer salts, e.g. κ -(BEDT-TTF)₂X. They can be modelled in terms of an effective Hamiltonian that is a single band Hubbard model on an anisotropic triangular lattice at half filling [5]. As the pressure increases these materials undergo a first order phase transition from a Mott insulator to a Fermi liquid metal. Near the critical point, some signatures of critical behaviour have been reported in the conductivity [13, 39] and NMR [40]. Powell, Yusuf, and McKenzie [41] reviewed experimental NMR data on κ -(BEDT-TTF)₂X. In general it is found that in both the Mott insulating and metallic phases that above some temperature T_{NMR} at which $1/(T_1T)$ is a maximum that $1/T_1 = bT/(T + T_b)$ where b is a constant. Hence, above some temperature of the order $T_b \sim 50$ K, the NMR relaxation rate becomes roughly independent of temperature. Broadly, this is consistent with the quantum criticality discussed here. On the other hand, there are alternative explanations in terms of short-range antiferromagnetic spin fluctuations [41], and the experiments cover a relatively narrow temperature range, roughly 50-300 K, which is not even a single decade. Our results compare well qualitatively with experimental results for κ -(BEDT-TTF)₄Hg_{2.89}Br₈ (see Figure 3(c) in Reference [42]). As the pressure increases $1/(T_1T)$ decreases by more than an order of magnitude. It smoothly crosses over from a form that is monotonically decreasing with temperature above about 10 K at low pressures to weak temperature dependence (Korringa) at higher pressures. In a range of organics the Korringa ratio is observed to be temperature dependent with large values of order ten [43, 44]. We hope our results will stimulate

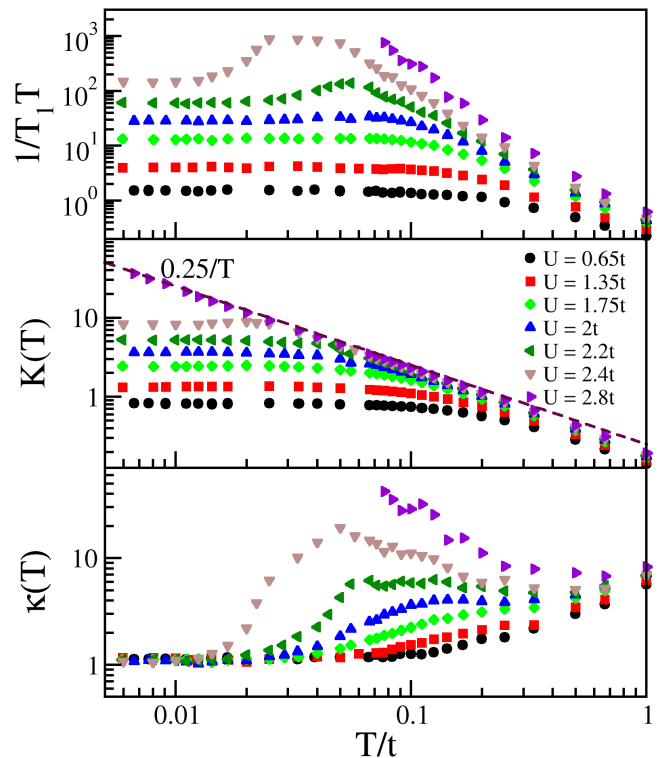


Figure 4. Temperature dependence of NMR properties for a range of U values. The top panel shows the Nuclear spin relaxation rate, $1/T_1T$. The middle panel shows the local static susceptibility (Knight shift) Note that both quantities are significantly enhanced as the Mott transition is approached on the metallic site. Below the coherence temperature T_{coh} , both are independent of temperature, characteristic of a Fermi liquid. Well above T_{coh} the static susceptibility approaches the Curie form ($\chi = 1/(4T)$), shown by the purple dashed line), suggesting unscreened local moments. The bottom panel shows the Korringa-Shiba ratio, defined in Eqn. (3). Below T_{coh} it approaches one, and above T_{coh} it is larger than one and increases with U .

new experiments.

It is also interesting to speculate if this QCP could be related to that found at finite doping in the 2D Hubbard model using Dynamical Cluster QMC simulations[45, 46]. Here the QCP separates the pseudogap and Fermi liquid regions, with a large region of ω/T marginal Fermi liquid[14] scaling above the QCP. Calculations are now underway to explore this possibility.

Conclusions. We have provided a concrete example of a fermion model which has a metallic state in proximity to a Mott insulating state and has dynamical local spin fluctuations that exhibit the ω/T scaling that is characteristic of quantum criticality.

Acknowledgments. ND thanks CSIR and DST (India) for research funding. RHM was supported in part by an Australian Research Council Discovery Project. He also benefited from discussions at the Aspen Center for Physics, which is supported by National Science Foundation grant PHY-1066293. We thank Vladimir Dobrosavljevic, Jure

Kokalj, Alejandro Mezio, Peter Prelovsek, Qimao Si, Darko Tanaskovic, and Rok Zitko for helpful discussions. Our simulations used an open source implementation [47] of the hybridization expansion continuous-time quantum Monte Carlo algorithm [48] and the ALPS [49] libraries. The computational resources are provided by the Louisiana Optical Network Initiative (LONI) and HPC@LSU.

* nagamalleswararao.d@gmail.com

† r.mckenzie@uq.edu.au; URL: condensedconcepts.blogspot.com

- [1] M. Imada, A. Fujimori, and Y. Tokura, *Reviews of Modern Physics* **70**, 1039 (1998)
- [2] B. Keimer, S. Kivelson, M. Norman, S. Uchida, and J. Zaanen, *Nature* **518**, 179 (2015)
- [3] J. G. Analytis, H. Kuo, R. D. McDonald, M. Wartenbe, N. Hussey, and I. Fisher, *Nature Physics* **10** (2014)
- [4] P. Gegenwart, Q. Si, and F. Steglich, *Nature Physics* **4**, 186 (2008)
- [5] B. Powell and R. H. McKenzie, *Reports on Progress in Physics* **74**, 056501 (2011)
- [6] S. Sachdev, *Quantum phase transitions*, 1st ed. (Cambridge, 1999)
- [7] S. Sachdev, *Science* **288**, 475 (2000)
- [8] S. Sachdev and B. Keimer, *Physics Today* **64**, 29 (2011)
- [9] A. Georges, G. Kotliar, W. Krauth, and M. J. Rozenberg, *Reviews of Modern Physics* **68**, 13 (1996)
- [10] H. Terletska, J. Vučićević, D. Tanasković, and V. Dobrosavljević, *Physical Review Letters* **107**, 026401 (2011)
- [11] J. Vučićević, H. Terletska, D. Tanasković, and V. Dobrosavljević, *Physical Review B* **88**, 075143 (Jan. 2013)
- [12] J. Vučićević, D. Tanasković, M. Rozenberg, and V. Dobrosavljević, *Physical Review Letters* **114**, 246402 (2015)
- [13] T. Furukawa, K. Miyagawa, H. Taniguchi, R. Kato, and K. Kanoda, *Nature Physics* **11**, 221 (2015)
- [14] C. Varma, P. B. Littlewood, S. Schmitt-Rink, E. Abrahams, and A. Ruckenstein, *Physical Review Letters* **63**, 1996 (1989)
- [15] C. M. Varma, *Reports on Progress in Physics* **79**, 082501 (2016)
- [16] O. Parcollet and A. Georges, *Physical Review B* **59**, 5341 (1999)
- [17] B. Lake, D. A. Tennant, C. D. Frost, and S. E. Nagler, *Nature materials* **4**, 329 (2005)
- [18] J. S. Helton, K. Matan, M. P. Shores, E. A. Nytko, B. M. Bartlett, Y. Qiu, D. G. Nocera, and Y. S. Lee, *Phys. Rev. Lett.* **104**, 147201 (Apr 2010)
- [19] L. Zhu, S. Kirchner, Q. Si, and A. Georges, *Physical Review Letters* **93**, 267201 (Dec. 2004)
- [20] S. Kirchner and Q. Si, *Phys. Rev. Lett.* **100**, 026403 (Jan 2008)
- [21] A. Schröder, G. Aeppli, R. Coldea, M. Adams, O. Stockert, H. Löhneysen, E. Bucher, R. Ramazashvili, and P. Coleman, *Nature* **407**, 351 (2000)
- [22] P. Werner and A. J. Millis, *Phys. Rev. B* **75**, 085108 (Feb 2007)
- [23] E. Gull, A. J. Millis, A. I. Lichtenstein, A. N. Rubtsov, M. Troyer, and P. Werner, *Reviews of Modern Physics* **83**, 349 (2011)
- [24] M. Jarrell and J. E. Gubernatis, *Physics Reports* **269**, 133 (1996)
- [25] M. Jarrell, J. E. Gubernatis, and R. N. Silver, *Phys. Rev. B* **44**, 5347 (Sep 1991)
- [26] M. Salomaa, *Zeitschrift für Physik B* **25**, 49 (1976)
- [27] K. Bouadim, Y. L. Loh, M. Randeria, and N. Trivedi, *Nature Physics* **7**, 884 (2011)
- [28] J. Kokalj and R. McKenzie, *Physical Review Letters* **110**, 206402 (May 2013)
- [29] X. Deng, J. Mravlje, R. Žitko, M. Ferrero, G. Kotliar, and A. Georges, *Phys. Rev. Lett.* **110**, 086401 (Feb 2013)
- [30] S. Sanyal and M. Eckstein, *Phys. Rev. Lett.* **117**, 096403 (Aug 2016)
- [31] C. Raas and G. S. Uhrig, *Physical Review B* **79**, 115136 (Jan. 2009)
- [32] I. Affleck, arXiv preprint cond-mat/9512099(1995)
- [33] S. Sachdev, *Physical Review Letters* **105**, 151602 (2010)
- [34] N. Dasari, S. Acharya, A. Taraphder, J. Moreno, M. Jarrell, and N. Vidhyadhiraja, arXiv preprint arXiv:1509.09163(2015)
- [35] K. Kitagawa, K. Ishida, R. S. Perry, T. Tayama, T. Sakakibara, and Y. Maeno, *Phys. Rev. Lett.* **95**, 127001 (2005)
- [36] R. Zitko, Z. Osolin, and P. Jeglic, *Phys. Rev. B* **91**, 155111 (2015)
- [37] E. Yusuf, B. Powell, and R. H. McKenzie, *Journal of Physics: Condensed Matter* **21**, 195601 (2009)
- [38] H. Shiba, *Progress of Theoretical Physics* **54**, 967 (1975)
- [39] F. Kagawa, K. Miyagawa, and K. Kanoda, *Nature* **436**, 534 (2005)
- [40] F. Kagawa, K. Miyagawa, and K. Kanoda, *Nature Physics* **5**, 880 (2009)
- [41] B. J. Powell, E. Yusuf, and R. H. McKenzie, *Physical Review B* **80**, 054505 (Aug. 2009)
- [42] Y. Eto, M. Itaya, and A. Kawamoto, *Phys. Rev. B* **81**, 212503 (2010)
- [43] S. M. De Soto, C. P. Slichter, A. M. Kini, H.-H. Wang, U. Geiser, and J. Williams, *Physical Review B* **52**, 10364 (1995)
- [44] M. Itaya, Y. Eto, A. Kawamoto, and H. Taniguchi, *Physical Review Letters* **102**, 227003 (2009)
- [45] N. S. Vidhyadhiraja, A. Macridin, C. Sen, M. Jarrell, and M. Ma, *Phys. Rev. Lett.* **102**, 206407 (2009)
- [46] E. Khatami, K. Mielsonson, D. Galanakis, A. Macridin, J. Moreno, R. T. Scalettar, and M. Jarrell, *Phys. Rev. B* **81**, 201101 (2010)
- [47] H. H. Hafermann, P. Werner, and E. Gull, *Computer Physics Communications*, 184, 1280 (2013)
- [48] P. Werner, A. Comanac, L. de' Medici, M. Troyer, and A. J. Millis, *Phys. Rev. Lett.* **97**, 076405 (Aug 2006)
- [49] B. Bauer et al, *Journal of Statistical Mechanics: Theory and Experiment*, 2011, P05001 (2011)

Supplemental Material: Quantum critical local spin dynamics near the Mott metal-insulator transition in infinite dimensions

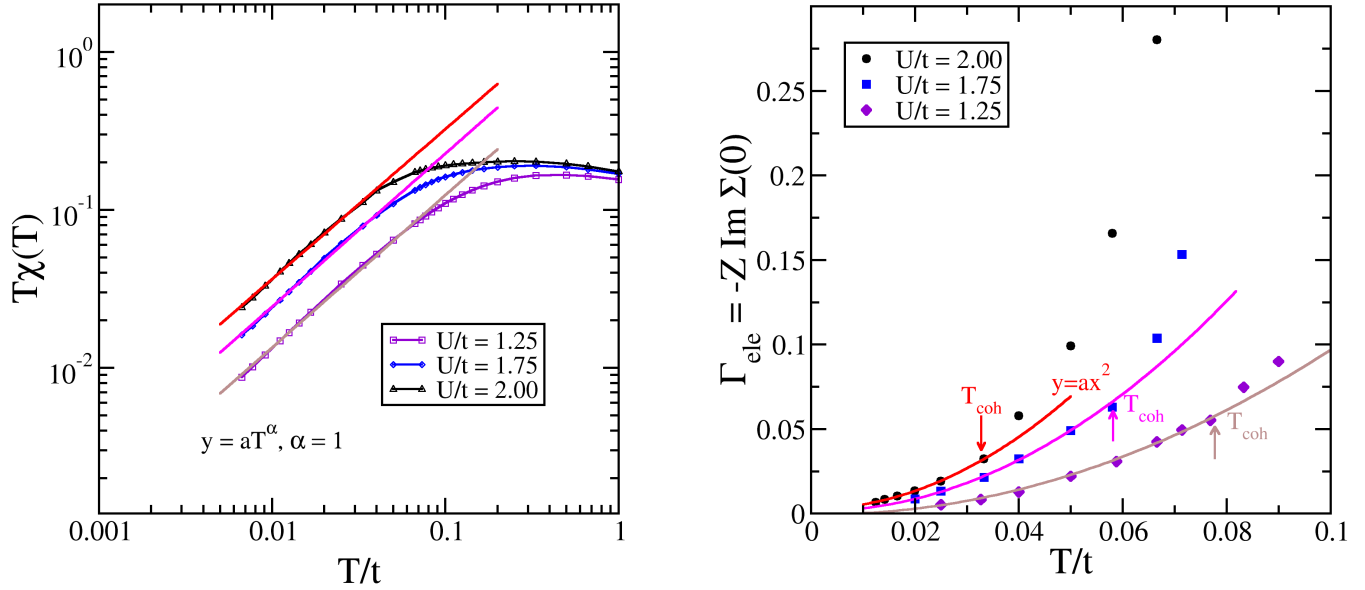


Figure S1. Determination of the Fermi liquid coherence temperature. Right panel: from the static local spin susceptibility, T_{coh} is defined as the temperature at which $\chi(T)$ deviates from the temperature independence characteristic of a Fermi liquid. Left panel: from the self energy for the one-electron Green's, T_{coh} is defined as the temperature at which $\Sigma''(\omega = 0, T)$ deviates from the quadratic temperature dependence characteristic of a Fermi liquid.

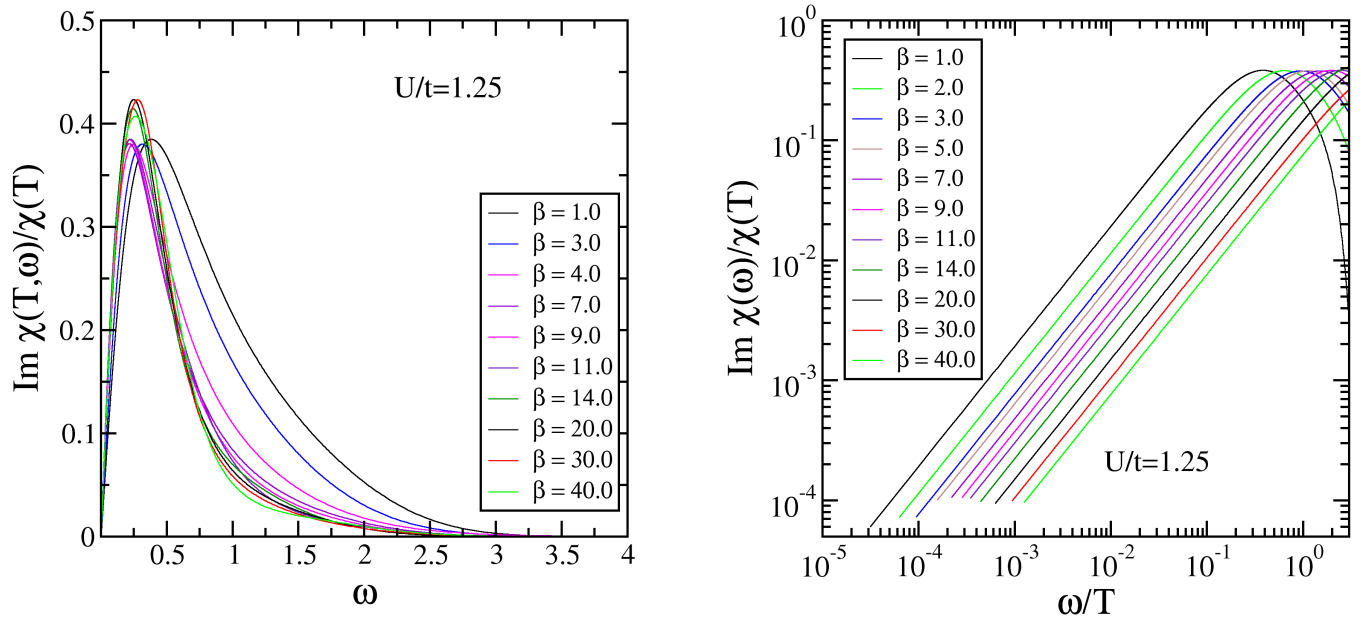


Figure S2. Frequency dependence of the dynamical spin susceptibility in the metallic phase. The right panel shows the frequency dependence of the imaginary part of the susceptibility for $U/t=1.25$ for a range of temperatures and on a linear scale. The left panel shows the same data on a log-log plot with the frequency scaled by temperature. Unlike in the quantum critical regime, ω/T scaling is not observed.

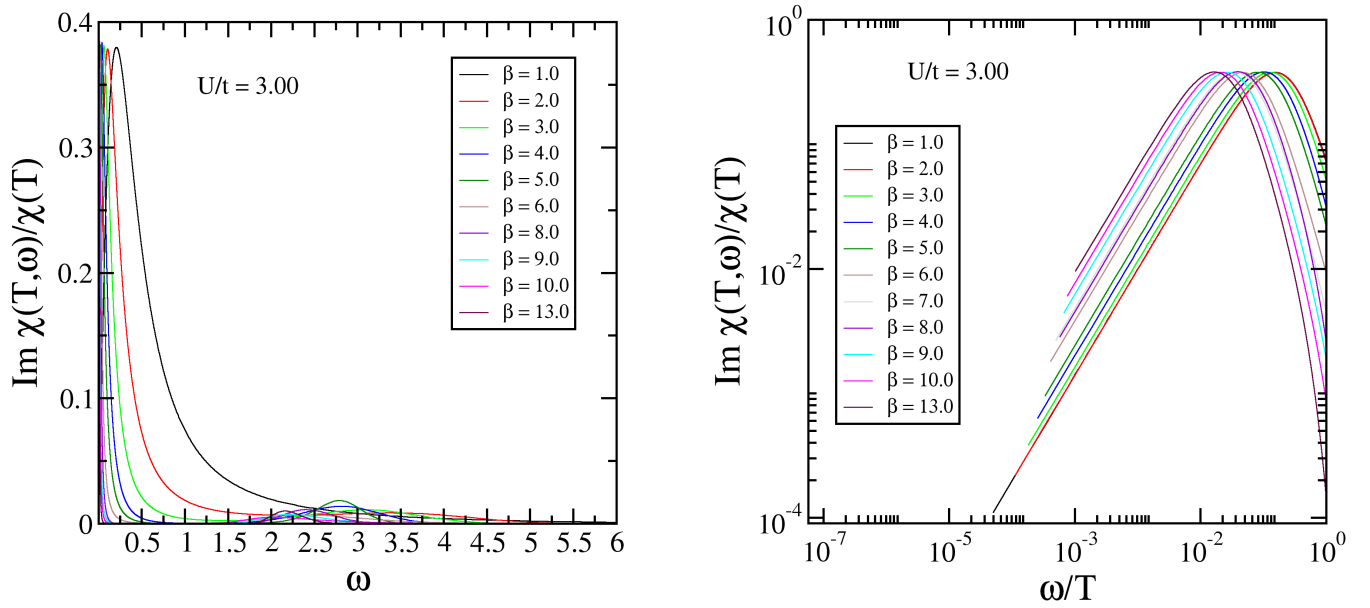


Figure S3. Frequency dependence of the dynamical spin susceptibility in the Mott insulating phase. The right panel shows the frequency dependence of the imaginary part of the susceptibility for $U/t=3.0$ for a range of temperatures and on a linear scale. Note how as the temperature tends to zero the peak width tends to zero and that one sees features around $\omega = U$, associated with the Hubbard bands. The left panel shows the same data on a log-log plot with the frequency scaled by temperature. Unlike in the quantum critical regime, ω/T scaling is not observed.

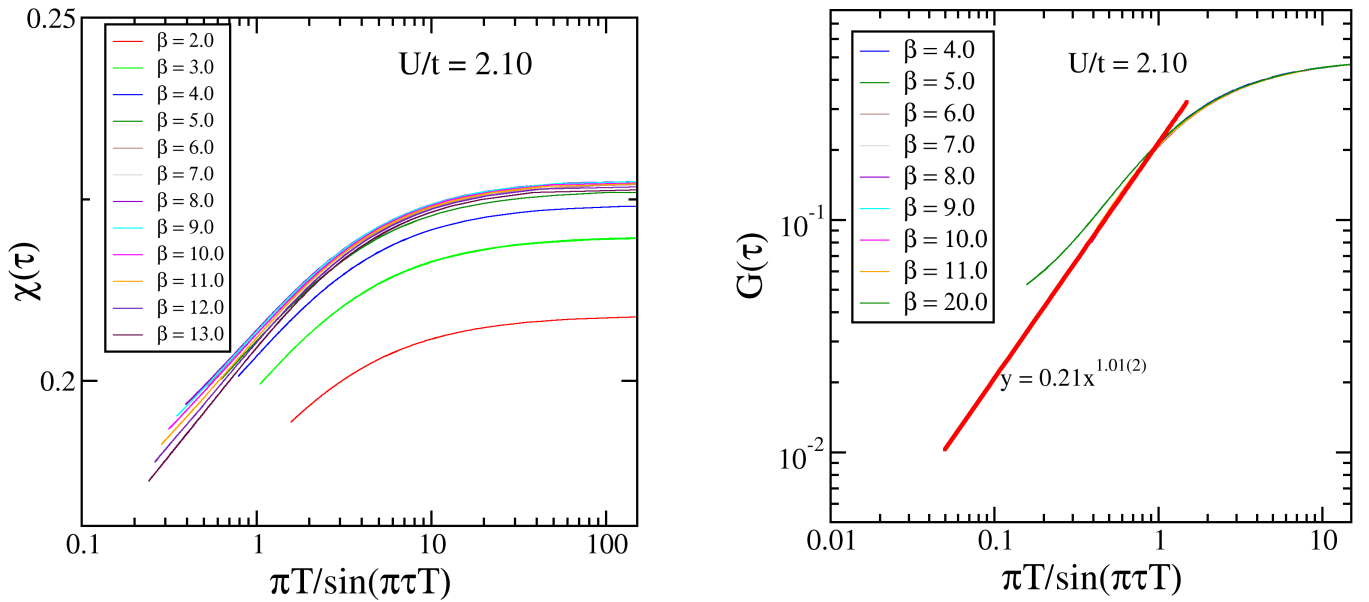


Figure S4. The right panel shows the failure of Boundary Conformal Field Theory scaling of the imaginary time dependence of the susceptibility $\chi(\tau)$. The left panel shows the Boundary Conformal Field Theory scaling of the imaginary time dependence of the one electron Green's function, $G(\tau)$. Curves are shown for $U = 2.10t$ and for a range of temperatures ($\beta = 1/T$).

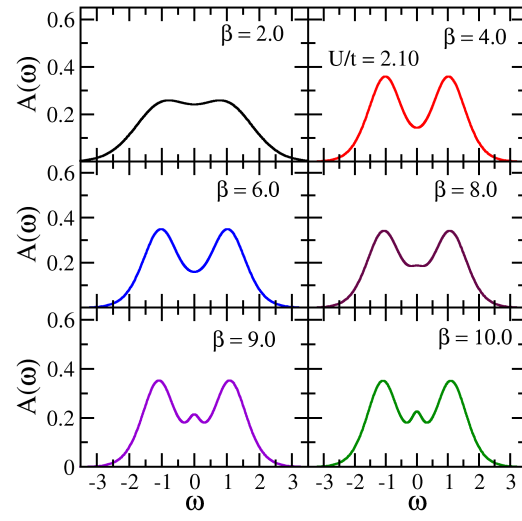


Figure S5. One electron spectral density for $U/t = 2.10$ for different temperatures in the quantum critical region. Compare Fig. 7 in Ref. S11. The bad metal is defined by the absence of the quasi-particle peak at $\omega = 0$.